2017 25th Mediterranean Conference on Control and Automation (MED)
July 3-6, 2017. Valletta, Malta

Bearing only visual homing: Observer based approach

Misha Gupta, Arunkumar G.K and Leena Vachhani

Abstract— **Many robotic applications such as pick and place, navigation, docking, etc. need to visit a known place as an intermediate task. Homing is a method to reach a known position and is challenging to address specially in a GPS denied indoor environment. The approach is to match the information collected at home and current locations. The information collected from images is rich in amount, however to extract the relevant information from images is challenging. This paper solves the homing problem using bearing only measurements as this information can be easily extracted from the features in an image. The observable system shows that the bearing only measurements avoid the need to know the locations of landmarks and instantaneous distance of the robot with respect to the home position. Instantaneous state of the robot is estimated using EKF (Extended Kalman Filter). Simulation results with real images from two data-sets show that the estimation of the robot's state is of the order of 10^{-2} cm in range, 10^{-2} radians in bearing and 10^{-16} radians in orientation. Comparison with existing visual homing techniques show that the proposed technique has faster convergence of the robot's position to the home position due to good estimates.**

Index Terms— **homing, bearing only visual homing, observer, nonlinear system, panoramic image**

I. Introduction

Homing is the task of returning the robot to a predefined 'home' or reference position accurately from a nearby location. It is an important intermediate sub-task in many applications such as indoor and outdoor navigation, tracking, docking of the robots, formation of swarm robots, etc. The key is to collect information about relative position and orientation of the robot with respect to home position and reference direction. Achieving this task using one kind of sensor for a low-cost small-sized mobile robot moving in GPS denied indoor environment is challenging. We consider collecting panoramic images for feedback. Capability to resolve ambiguity is the main advantage in visual sensing over other typical sensors used in robotics such as ultrasonic, laser, etc. Although visual data gives enormous information about the environment, the challenge lies in extracting the pertinent information for homing of the robot.

Visual homing requires using a monocular camera as feedback system. [1], [2] is robust and flexible since the robot can correct motion errors if arise by aligning current image with respect to target image. The autonomous robot captures image at the home position (on its first visit or offline) in visual homing. This image is compared with that obtained at the current position. Panaromic sensor support vision based tasks for environments [3], [4] that lack rich visual content, increasing the probability of identifying features that are suitable for supporting navigation. Bearing only method incorporating feature extraction and matching [5]–[7] is used to set up correspondence vectors between the current and the target images for known orientation of the robot. The average landmark vector is estimated in [8], [9] using difference between bearings at reference and current positions.

The visual homing is also considered as a sub-problem of visual servoing [10]. The method however requires range information of landmarks (features) with respect to the home position. In practice, this information can be approximated with constant ranges, estimated by creating a map of the landmarks on-line [11], through the use of adaptive control [12] or using the relative scale of feature point descriptors [13]. A visual homing framework [14] based on the scale and bearing measurements of visual features uses Scale Invariant Feature Transform (SIFT). The convergence has been proved using Lyapunov method, but controller requires both scale and bearing information. Authors in [15] used a sliding-mode control law to exploit the epipolar geometry. The performance [16] has been improved using 1-D trifocal tensor from omnidirectional camera. Homing with Stereo-Vision [17] utilizes a stereo camera to build composite wide-field stereo images and estimate distance and bearing from the robot to home location. A Lyapunov based steering control strategy [18] for visual homing of mobile robots has been developed based on the correlation between images obtained at current and home positions which relates to the distance with respect to the home position.

We also relate the bearing only homing to the triangulation using known locations of landmarks. Various triangulation techniques to estimate position using three landmark positions are compared [19] in terms of robustness and computation time. The mobile robot localization [20], [21] has been achieved using triangulation technique. Algorithm for optimal selection of landmark positions [22] has also been developed. An efficient triangulation method and an off-the-shelf landmark bearing sensor [23] has been developed to a complete localization system. The EKF based estimation and consistent triangulation [24] has been developed for mobile robot localization. An optimization approach [25] to bearing-only visual homing with landmarks uses control law based on gradient field. A single landmark based localization algorithm [26] uses landmark information in three dimension which is not possible with only one image sensor. It is worth noting that only the bearing information of landmarks (features in the image) is available in visual homing with monocular camera as against both range and bearing information in triangulation unless size of the landmark is known.

In this work, we investigate bearing only method for estimating position with respect to the home position. Our approach involves model based mobile robot homing using bearing only measurements from images. Following are the key contributions of this paper: In the proposed method,

- Only the bearing angles to the landmarks are used to estimate state of the system (the robot's position and

978-1-5090-4533-4/17/$31.00 ©2017 IEEE

orientation with respect to the home position and reference direction). Observability of this extended system is shown to substantiate the above claim. Extended Kalman Filter (EKF), as an observer is used to demonstrate the proposed state estimation.

- Proposed algorithm requires neither any prior information about the landmarks nor instantaneous ranges to landmarks. Moreover, uncalibrated panoramic camera is considered.
- Simulation results under ideal conditions and with real images from two data-sets validate the technique presented in this paper. Simulations show that the good state estimation using proposed algorithm and faster convergence with both proportional and nonlinear controllers as compared to existing techniques.

The rest of the paper is organized as follows. Next section formulates the problem addressed in this work. System observability analysis and proposed homing technique are described in section III. Section IV shows that the estimations match with the true values under ideal conditions as well as with real images. Section IV also compares convergence time of proposed algorithm with existing visual homing techniques. Conclusions and future directions of this work are presented in section V.

II. Problem formulation

The unicycle vehicle moving in a 2-D plane with constant linear velocity is considered for analysis. Figure 1 is used to describe the system. The control u of the robot is achieved by changing the angular velocity. The home position is denoted by H. Without loss of generality the home position is the origin of the reference frame X-Y. The current position of the robot at time instant t is marked by C. The line joining the home position (H) and current position (C) at time t is termed as instantaneous Line-of-Site (LoS). The positions of three landmarks are marked as L_1, L_2 and L_3 in Figure 1. Bearing angles to landmarks with reference to positive X-axis at home position (H) is denoted as $\theta_1^*, \theta_2^*, \theta_3^*$ which are calculated by capturing image at H. These values are stored as reference values. At the current position, the bearings of the landmarks with respect to the instantaneous velocity vector $\vec{v}$ is denoted as $\theta_1, \theta_2, \theta_3$. These measured bearing angles are calculated from the image captured at that position. The position of the robot in two dimensional plane is described using polar coordinates (R, θ), where R is the LoS distance from home position when origin is located at point H and θ is the bearing angle with respect to positive X-axis. The instantaneous orientation of the robot is denoted by α. All the angles are considered as positive in anti-clockwise direction. The visual homing system is described via the following system states:

$$X = \begin{cases} R : \text{radial distance from (C) to (H)} \\ \theta : \text{bearing angle of the robot} \\ \alpha : \text{orientation of the robot} \\ \theta_1 : \text{angle between line } L_1C \text{ and } \vec{v} \\ \theta_2 : \text{angle between line } L_2C \text{ and } \vec{v} \\ \theta_3 : \text{angle between line } L_3C \text{ and } \vec{v} \end{cases}$$

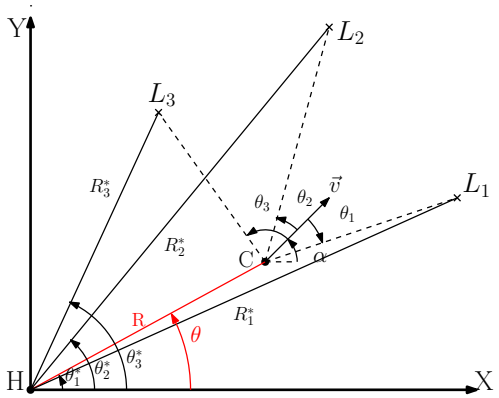

Fig. 1: Illustration for describing system

The unicycle model [18] is given by

$$\dot{R} = v\cos(\alpha - \theta), \qquad R\dot{\theta} = v\sin(\alpha - \theta) \tag{1}$$

where v is linear velocity of the robot. Let R_1^*, R_2^* and R_3^* be the ranges of the landmarks L_1, L_2 and L_3 respectively at H. Applying the sine rule in the $\triangle CL_1H$, $\triangle CL_2H$, $\triangle CL_3H$, we get

$$\frac{R}{\sin(\theta_i^* - (\theta_i + \alpha))} = \frac{R_i^*}{\sin(\pi - (\theta - (\theta_i + \alpha)))}, \tag{2}$$

$$R_i^* = R\frac{\sin(\theta - (\theta_i + \alpha))}{\sin(\theta_i^* - (\theta_i + \alpha))} \tag{3}$$

for each $i = 1, 2, 3$. It is worth noting that R_i^* for each $i = 1, 2, 3$ are constants, however they are not measured quantities. The rate of change of θ_i with respect to time t using (1) and (3) is given by,

$$\dot{\theta}_i = \frac{-v\sin(\theta_i)}{R\cos(\theta - (\theta_i + \alpha)) - R_i^*\cos(\theta_i^* - (\theta_i + \alpha))} - \dot{\alpha} \tag{4}$$

where R_i^* used in (4) is given by (3). For the purpose of conciseness, $\cos(\theta - (\theta_i + \alpha))$, $\cos(\theta_i^* - (\theta_i + \alpha))$, $\sin(\theta - (\theta_i + \alpha))$, $\sin(\theta_i^* - (\theta_i + \alpha))$, $\sin(\theta_i)$, $\cos(\theta_i)$ is taken as C_i, C_i^*, S_i, S_i^*, s_i, c_i respectively. From (1) and (4) the state space model of the system consisting of robot states and landmark bearing angles is described by $\dot{X} = g(X)u$, $X = \begin{bmatrix} R & \theta & \alpha & \theta_1 & \theta_2 & \theta_3 \end{bmatrix}^T$ where $u = [v \ \omega]^T$, ω is angular velocity of robot and g(X) is given by

$$g(X) = \begin{pmatrix} g_1 & g_2 \end{pmatrix} \tag{5}$$

$$= \begin{pmatrix} \cos(\alpha - \theta) & 0 \\ \frac{\sin(\alpha - \theta)}{R} & 0 \\ 0 & 1 \\ \frac{-\sin(\theta_1)}{RC_1 - R_1^*C_1^*} & -1 \\ \frac{-\sin(\theta_2)}{RC_2 - R_2^*C_2^*} & -1 \\ \frac{-\sin(\theta_3)}{RC_3 - R_3^*C_3^*} & -1 \end{pmatrix} \tag{6}$$

The output vector Y is given by

$$Y = \begin{pmatrix} \theta_1 & \theta_2 & \theta_3 \end{pmatrix}^T \tag{7}$$

III. Proposed observer based technique

System (6) consists of six states but only three states $\theta_1, \theta_2, \theta_3$ are measured from images. For controller design, current state of the robot with respect to the home position and reference direction is also required which are not measured using vision information. Problem can be resolved by estimating the robot's current state using current bearing measurements and system model. These estimations are obtained using an observer which can be used by control input to drive the robot, provided that the nonlinear system (6) is observable. State space model of system described by (6) and (7) is of the form

$$\dot{X} = g(X)u \qquad \text{and} \qquad Y = h(X) \tag{8}$$

Next, we find the local observability using Lie derivatives. Lie derivatives of the observation function over the control functions are given by (9), (11), (13). Following abbreviations are used for observability matrix representation. Let $(RC_i - R_i^* C_i^*)$,$\frac{s_i(C_i - \frac{C_i^* R_i^*}{R})}{d_i^2}$, $\frac{Rs_i(S_i + \frac{C_i C_i^*}{S_i^*})}{d_i^2}$, $\frac{-s_i C_i^*}{S_i^* d_i}$, $\frac{-c_i}{d_i} - \frac{s_i C_i^*}{S_i^* d_i}$ be d_i, J_i, K_i, P_i, Q_i respectively for any i=1, 2, 3. Observation matrices are:-

$$L^0 h = h(X) = \begin{pmatrix} \theta_1 & \theta_2 & \theta_3 \end{pmatrix}^T \tag{9}$$

$$\nabla L^0 h = \nabla h(X) = \begin{pmatrix} 0 & 0 & 0 & 1 & 0 & 0 \\ 0 & 0 & 0 & 0 & 1 & 0 \\ 0 & 0 & 0 & 0 & 0 & 1 \end{pmatrix} \tag{10}$$

For first order lie derivative of h with respect to g_1, we have as

$$\nabla L^1_{g_1} h = \begin{pmatrix} J_1 & K_1 & P_1 & Q_1 & 0 & 0 \\ J_2 & K_2 & P_2 & 0 & Q_2 & 0 \\ J_3 & K_3 & P_3 & 0 & 0 & Q_3 \end{pmatrix} \tag{11}$$

$$L^1_{g_2} h = \frac{\partial h(X)}{\partial X} . g_2 = \begin{pmatrix} -1 & -1 & -1 \end{pmatrix}^T \tag{12}$$

$$\nabla L^1_{g_2} h = \begin{pmatrix} 0 & 0 & 0 & 0 & 0 & 0 \\ 0 & 0 & 0 & 0 & 0 & 0 \\ 0 & 0 & 0 & 0 & 0 & 0 \end{pmatrix} \tag{13}$$

Now, Observability matrix O is given by

$$O = \begin{pmatrix} \nabla L^0 h \\ \nabla L^1_{g_1} h \\ \nabla L^2_{g_2} h \end{pmatrix} \tag{14}$$

The rank of matrix O described by (14) is six. States R, θ, α are locally observable, when bearings to landmarks are measured. Using observer technique, these non-measured states but observable states are estimated. We next describe the proposed algorithm to estimate the robot's state.

Without loss of generality, we assume that the robot captures an image at home position (H) with $\alpha = 0$. The bearing angles to landmarks is obtained from image at home position. These angles are stored as $\theta_1^*, \theta_2^*, \theta_3^*$. The algorithm is described using a flow chart in Figure 2. The algorithm begins with capturing panoramic image at the unknown current position. Bearing angles to landmarks $\theta_1, \theta_2, \theta_3$ at current position (C) is calculated using image processing. Extended Kalman Filter (EKF) is used as a choice of nonlinear observer. Successive local linearization is $G(k) = [\frac{\partial g}{\partial X}]_{\hat{X}(k-1|k-1), U(k-1)}$ where g and X are from system model (6). Predicted mean is $\hat{X}(k \mid k-1) = F(\hat{X}(k-1 \mid k-1), U(k-1))$ which is obtained from system model using ode. Predicted variance is $P(k \mid k-1) = G(k)P(k-1 \mid k-1)G(k)^T + Q$ where Q is process noise. Further, Kalman Gain is computed as L(k) with above prediction using $C(k) = [\frac{\partial h}{\partial X}]_{\hat{X}(k|k-1)}$ and $L(k) = P(k \mid k-1)C(k)^T[C(k)P(k \mid k-1)C(k)^T + M]^{-1}$ where M is measurement noise. Here,

$$C(k) = \begin{pmatrix} 0 & 0 & 0 & 1 & 0 & 0 \\ 0 & 0 & 0 & 0 & 1 & 0 \\ 0 & 0 & 0 & 0 & 0 & 1 \end{pmatrix} \tag{15}$$

States are updated using $e(k) = [Y(k) - C(k)\hat{X}(k \mid k-1)]$, $\hat{X}(k \mid k) = \hat{X}(k \mid k-1) + L(k)e(k)$ and $P(k \mid k) = [I - L(k)C(k)]P(k \mid k-1)$. Measurement angles are fused to this EKF update step which estimates unmeasured states (R, θ, α) using system model. $\hat{R}, \hat{\theta}, \hat{\alpha}$ are estimated states which are used by the controller and thereby desired angular velocity is given to the robot. The loop continues till $\theta_i^* - (\theta_i + \alpha)$ is close to zero i.e. when measured bearings to landmarks at current position are almost equal to the corresponding bearings at the home position. The bearings are equal only when the robot reaches home position (R approaches 0).

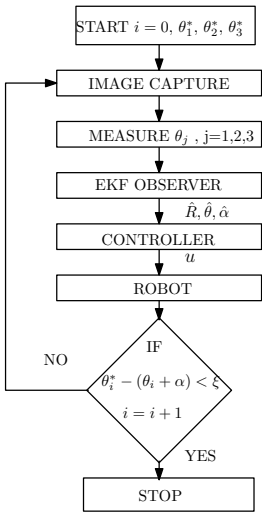

Fig. 2: Proposed homing algorithm

IV. Simulation Results

The proposed homing technique is simulated for following two cases: under ideal conditions and using real images. Under ideal conditions, the accurate bearing from the landmarks to current position of the robot is calculated by ode solver. The other simulation is performed with the data which is calculated from the images from image data-set [27] which uses multiple camera assembly as well as the images from Vardy's data-set [28] which uses camera and hyperbolic mirror assembly for collecting panoramic image. Algorithm is tested with two different control laws for homing using the information obtained from the panoramic images at current

and home positions. Proportional controller is $\omega = \pi - (\hat{\alpha} - \hat{\theta})$ where $\hat{\alpha}, \hat{\theta}$ are obtained from EKF. ω defines the steering control input at time t. Other controller is Lyapunov function based nonlinear control law which depends on the output of a signum function [18]. The input to the signum function is the change in $\hat{\theta}$. Nonlinear controller is

$$\omega = \beta \frac{v}{R_c} \text{sgn}(\dot{\hat{\theta}}), \forall \beta > 1 \tag{16}$$

where $\beta > 1$ is a free parameter, R_c is the radius of a circle centered at home position. The control-law steers the robot to asymptotically reach inside the circular area centered at home position with radius R_c. We next present the simulation results for homing using both the controllers when state is estimated using proposed observer technique.

A. Simulation under ideal condition

Various combination of initial positions and orientations covering each quadrant are considered to verify the algorithm presented in previous section. MATLAB 2014 is used for simulations. Landmarks are located at (150, 30), (100, 180), (20, 60) for simulation. The ode45 solver of MATLAB is used to compute the actual position and orientation of the robot at each sampling instant T_s to compare with estimated values. Sampling time T_s is 0.1 s and simulation is stopped when the robot reaches a circle of radius 5 cm ($R_c = 5$ cm) centered at home position. Process noise matrix is zero mean white noise with $Q = 0.01 I_{6\times6}$ where $I_{6\times6}$ is identity matrix of dimension six. Measurement noise is zero mean white noise with $M = 0.1 I_{3\times3}$. Initial co-variance $P(0 \mid 0)$ for the EKF is taken as $I_{6\times6}$ for ideal case. The linear velocity v is constant and equal to 12 cm/sec. The robot's path for four initial conditions, $P_1(x, y, \alpha)$ = (59, 42, -120°), P_2 = (-60, 40, 90°), P_3 = (-82, -68, 150°), P_4 = (32, -57, -40°) are shown in Figures 3a and 3b with proportional and nonlinear controllers respectively. Initial positions and orientations of the robot are shown using black squares and small arrows respectively. Home position is marked with red square marker. The initial conditions are unknown to the proposed algorithm and used for illustration purpose. It shows that robot is converging to home position (origin) from initial state using above algorithm with both nonlinear and proportional controllers. Error is calculated for estimated states with respect to actual values for both the cases. Table I shows error in estimated states for nonlinear and proportional

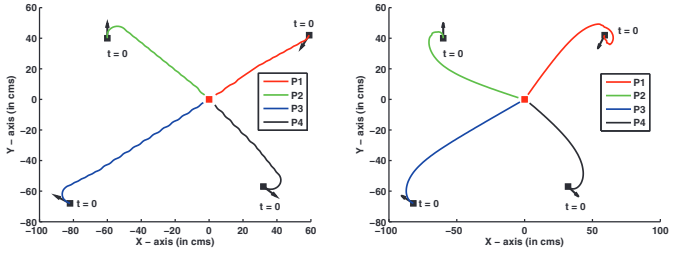

(a) Using nonlinear control (b) Using proportional control

Fig. 3: Path followed by the robot under ideal conditions

controllers. To demonstrate the relative performance of both control laws with algorithm, RMSE (Root Mean Squared Error) of estimated states w.r.t actual values is calculated. RMSE for each state value is calculated as

$$(RMSE)_i = \sqrt{\sum_{k=1}^{N} \frac{[x_i(k) - \hat{x}_i(k \mid k)]^2}{N}} \tag{17}$$

where N is the number of iterations to converge to home position, $x_i(k)$ is actual state and $\hat{x}_i(k \mid k)$ is estimated state. The contents of Table I shows that error in estimation with proposed algorithm for model is of the order of 10^{-3} cm in range, 10^{-4} radians in bearing and 10^{-16} radians in orientation.

B. Simulation with images from data-set

The algorithm is implemented on data obtained from image data-set. This data-set [27] contains images captured by differential drive mobile robot Fire Bird XI. The camera setup uses eight i-ball C12.0 web cameras to cover panoramic view. The optical axes of two adjacent cameras are co-planar and π/4 apart so that a significant overlapping is possible in images captured with two adjacent cameras. The panoramic image obtained from 8-camera setup is re-sized to 480×4680 for obtaining number of columns as integer multiple of 360. The images are captured at 9×19 grid elements within the free space of the indoor environment. Distance between each grid point is 29.25 cm. Grid element (5,10) is the home position. Reference Image at the home position is matched with images at all instants. Features are detected using Speeded Up Robust Features (SURF) and are matched using their descriptors following to which outliers are removed and object is detected. Objects or landmarks in reference image are matched with other images as shown in Figure 4. Center of detected objects is taken as landmark position. Image coordinate in x-direction at each instant is taken in terms of angle to landmarks. Bearing angle corresponding to detected feature is calculated as $2\pi x/l$ where l is length of panoramic image in pixels in x-direction and x is x-coordinate of detected feature. Landmark angle measurement in between grids is calculated by linear interpolation from the images at nearby grid points. In above case, l is 4680. Therefore 13 pixels corresponds to 1°. Figure 4 shows detected features in one of the intermediate image. Process noise considered is zero mean white noise with $Q = 0.01 I_{6\times6}$. Measurement noise is zero mean white noise with $M = I_{3\times3}$. Initial co-variance $P(0 \mid 0)$ for the EKF is $I_{6\times6}$. Algorithm is tested for both nonlinear control and proportional control. Sampling time is taken as 0.1s. The robot's path for various initial conditions, $P_1(x, y, \alpha)$ = (82, 60, -45°), P_2 = (-78, 33, -90°), P_3 = (-55, -40, 135°), P_4 = (62, -31, -110°) are

Fig. 4: A panoramic image at reference position from our image data-set [27]; Colored boxes show detected features

TABLE I: RMSE for simulation using accurate measurement

Initial position	$R - \hat{R}$**(cm)**		$\theta - \hat{\theta}$**(radians)**		$\alpha - \hat{\alpha}$**(radians)**	
	Proportional controller	nonlinear controller	Proportional controller	nonlinear controller	Proportional controller	nonlinear controller
P_1	0.03680	0.008	0.0497	5.077e-04	1.7229e-16	0
P_2	0.01672	4.0831e-04	0.0073	4.4109e-05	2.0192e-16	0
P_3	1.6756e-04	9.6656e-05	3.5633e-05	3.6028e-05	5.4060e-16	9.8646e-17
P_4	5.0917e-04	4.0893e-04	1.1741e-04	5.5575e-05	4.0341e-16	5.4664e-17

TABLE II: RMSE for simulation using our image data-set [27]

Initial position	$R - \hat{R}$**(cm)**		$\theta - \hat{\theta}$**(radians)**		$\alpha - \hat{\alpha}$**(radians)**	
	Proportional controller	nonlinear controller	Proportional controller	nonlinear controller	Proportional controller	nonlinear controller
P_1	0.0101	0.0343	0.0472	0.0252	1.2678e-16	0
P_2	0.08	0.035	0.06	0.012	3.0192e-16	0
P_3	0.0121	0.0412	0.0123	0.0236	2.6564e-17	7.0217e-18
P_4	0.1531	0.0249	0.0293	0.0137	2.0472e-17	1.9910e-16

shown in Figure 5a and 5b. It shows that the robot reaches to home position i.e. origin from initial state using proposed algorithm with both nonlinear control input and proportional controller for various initial positions and orientations. RMSE is computed using 17 for estimated states with respect to actual values for both controller cases. Table II shows errors in estimated states for nonlinear and proportional controllers. The contents of Table II shows that error in estimation with proposed algorithm is of the order of 10^{-2} cm in range, 10^{-2} radians in bearing and 10^{-16} radians in orientation.

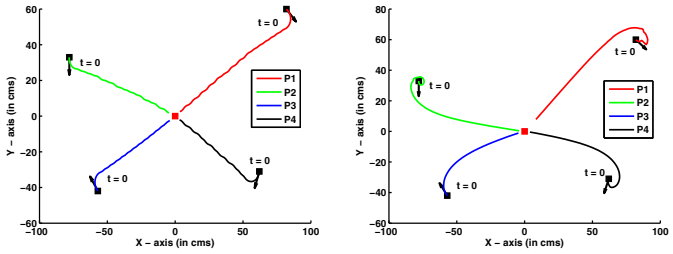

(a) Using nonlinear control (b) Using proportional control

Fig. 5: Path followed by robot for our image data-set [27]

Vardy's image data-set [28] for algorithm validation is also used for simulation. data-set provides panoramic images captured by a camera and hyperbolic mirror assembly at various grid positions. The images have been captured at each grid position separated by 30 cm over a grid of 10×17. Each panoramic image is of size 81×561. Figure 6 shows the image from the data-sets captured at grid position (4,8) i.e. home position. The robot's path for different initial positions, $P_1(x, y, \alpha)$ = (159, 108, 15°), P_2 = (-150, 95, 160°), P_3 = (-140, -102, 30°), P_4 = (134, -140, -130°) are shown in Figure 7a and 7b. The robot reaches to the home position in different initial conditions using both the controllers. Error in estimation is of the same magnitude as in the case of our image data-set.

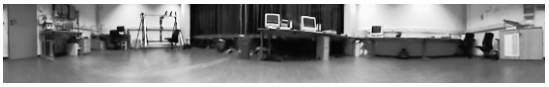

Fig. 6: A Panoramic image from Vardy's data-set [28]

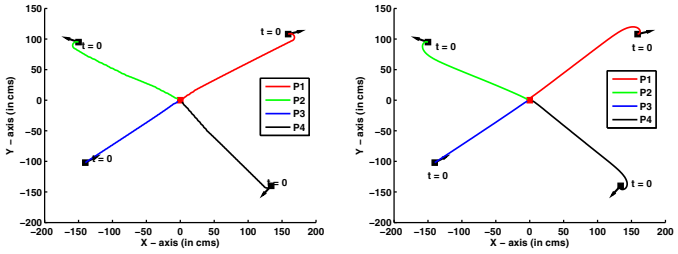

(a) Using nonlinear control (b) Using proportional control

Fig. 7: Path followed by the robot for Vardy's image data-set [28]

C. Comparison with other techniques

The proposed algorithm is compared with visual homing algorithms existing in literature. These algorithms [6], [9] are simulated using the images from data-set [27] which uses a multiple camera assembly as well as using the images from Vardy's data-set [28]. Convergence times for visual homing algorithms are simulated under same initial conditions. Simulation results are presented under four different initial positions in Figures 8a and 8b. Figure 8a gives comparison of convergence time in homing using images from data-set [27] for proposed algorithm with proportional controller, proposed algorithm with nonlinear controller, bearing only method [6] and ALV mehod [9]. Similiar comparison is done in Figure 8b of convergence time using Vardy's data-set [28]. The initial conditions considered for simulation in Figure 8 using image data-set collected from multiple camera assembly [27] are same as those used in section IV-B. Sampling time, T_s is

10 ms and linear velocity for proposed algorithm is 10 cm/s. For comparison purposes, the linear velocities are scaled properly to maintain nominal velocity of 10 cm/s. Figures 8a and 8b illustrates that the time taken for convergence to home position (0,0) is always less in proposed technique with different controllers as compared to that in existing methods. Faster convergences using proportional as well as nonlinear controller are due to good state estimation rendered by the proposed algorithm.

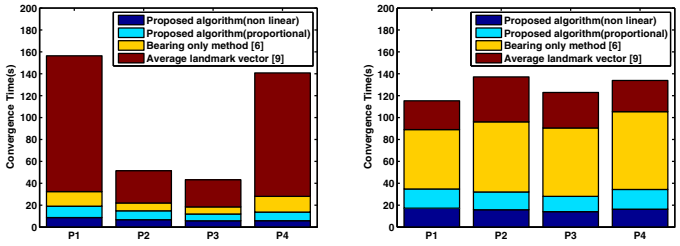

(a) Using our data-set [27] (b) Using Vardy's data-set [28]

Fig. 8: Comparison of proposed method with other methods

V. Conclusion and Future work

Observing the robot's current position and orientation with respect to the home position and reference direction is possible using bearing only measurements. The state estimation using a nonlinear observer (such as EKF) show faster convergence as compared to the existing visual homing techniques. Proposed technique also show that monocular images can be used for state estimation. The proposed observer based technique is also applicable to triangulation method for localization where landmark locations are also known. Simulations using real images from two data-sets have shown promising results. Future work involves experiments with the mobile robot for navigating the robot through predefined way-points using the proposed visual homing technique.

Acknowledgment

This work is supported by `flipkart.com`

References

[1] B. Espiau, F. Chaumette, and P. Rives, "A new approach to visual servoing in robotics," *IEEE Transactions on Robotics and Automation*, vol. 8, no. 3, pp. 313–326, 1992.

[2] G. N. DeSouza and A. C. Kak, "Vision for mobile robot navigation: A survey," *IEEE transactions on pattern analysis and machine intelligence*, vol. 24, no. 2, pp. 237–267, 2002.

[3] A. A. Argyros, K. E. Bekris, S. C. Orphanoudakis, and L. E. Kavraki, "Robot homing by exploiting panoramic vision," *Autonomous Robots*, vol. 19, no. 1, pp. 7–25, 2005.

[4] K. E. Bekris, A. A. Argyros, and L. E. Kavraki, "Exploiting panoramic vision for bearing-only robot homing," in *Imaging beyond the pinhole camera*, pp. 229–251, Springer, 2006.

[5] T. Krajník, J. Faigl, V. Vonásek, K. Košnar, M. Kulich, and L. Přeučil, "Simple yet stable bearing-only navigation," *Journal of Field Robotics*, vol. 27, no. 5, pp. 511–533, 2010.

[6] M. Liu, C. Pradalier, Q. Chen, and R. Siegwart, "A bearing-only 2D/3D-homing method under a visual servoing framework," in *Robotics and Automation (ICRA), 2010 IEEE International Conference on*, pp. 4062–4067, IEEE, 2010.

[7] J. Lim, N. Barnes, *et al.*, "Robust visual homing with landmark angles.," in *Robotics: Science and Systems*, Citeseer, 2009.

[8] C. Angulo and L. Godo, "Using the average landmark vector method for robot homing," *Artificial Intelligence Research and Development*, vol. 163, p. 331, 2007.

[9] A. Ramisa, A. Goldhoorn, D. Aldavert, R. Toledo, and R. L. de Mantaras, "Combining invariant features and the ALV homing method for autonomous robot navigation based on panoramas," *Journal of Intelligent & Robotic Systems*, vol. 64, no. 3, pp. 625–649, 2011.

[10] P. Corke, "Mobile robot navigation as a planar visual servoing problem," in *Robotics Research*, pp. 361–372, Springer, 2003.

[11] T. Goedemé, T. Tuytelaars, L. Van Gool, D. Vanhooydonck, E. Demeester, and M. Nuttin, "Is structure needed for omnidirectional visual homing?," in *2005 International Symposium on Computational Intelligence in Robotics and Automation*, pp. 303–308, IEEE, 2005.

[12] N. P. Papanikolopoulos and P. K. Khosla, "Adaptive robotic visual tracking: Theory and experiments," *IEEE Transactions on Automatic Control*, vol. 38, no. 3, pp. 429–445, 1993.

[13] M. Liu, C. Pradalier, F. Pomerleau, and R. Siegwart, "Scale-only visual homing from an omnidirectional camera," in *Robotics and Automation (ICRA), 2012 IEEE International Conference on*, pp. 3944–3949, IEEE, 2012.

[14] M. Liu, C. Pradalier, and R. Siegwart, "Visual homing from scale with an uncalibrated omnidirectional camera," *IEEE Transactions on Robotics*, vol. 29, no. 6, pp. 1353–1365, 2013.

[15] H. M. Becerra, G. López-Nicolás, and C. Sagüés, "A sliding-mode-control law for mobile robots based on epipolar visual servoing from three views," *IEEE Transactions on Robotics*, vol. 27, no. 1, pp. 175–183, 2011.

[16] H. M. Becerra, G. López-Nicolás, and C. Sagüés, "Omnidirectional visual control of mobile robots based on the 1-D trifocal tensor," *Robotics and Autonomous Systems*, vol. 58, no. 6, pp. 796–808, 2010.

[17] P. Nirmal and D. M. Lyons, "Homing with stereovision," *Robotica*, pp. 1–18, 2015.

[18] A. Sabnis, L. Vachhani, and N. Bankey, "Lyapunov based steering control for visual homing of a mobile robot," in *Control and Automation (MED), 2014 22nd Mediterranean Conference of*, pp. 1152–1157, IEEE, 2014.

[19] C. J. Cohen and F. V. Koss, "Comprehensive study of three-object triangulation," in *Applications in Optical Science and Engineering*, pp. 95–106, International Society for Optics and Photonics, 1993.

[20] C. D. Mcgillem and T. S. Rappaport, "A beacon navigation method for autonomous vehicles," *IEEE Transactions on Vehicular Technology*, vol. 38, no. 3, pp. 132–139, 1989.

[21] M. Betke and L. Gurvits, "Mobile robot localization using landmarks," *IEEE transactions on robotics and automation*, vol. 13, no. 2, pp. 251–263, 1997.

[22] C. B. Madsen and C. S. Andersen, "Optimal landmark selection for triangulation of robot position," *Robotics and Autonomous Systems*, vol. 23, no. 4, pp. 277–292, 1998.

[23] I. Loevsky and I. Shimshoni, "Reliable and efficient landmark-based localization for mobile robots," *Robotics and Autonomous Systems*, vol. 58, no. 5, pp. 520–528, 2010.

[24] J. M. Font-Llagunes and J. A. Batlle, "Consistent triangulation for mobile robot localization using discontinuous angular measurements," *Robotics and Autonomous Systems*, vol. 57, no. 9, pp. 931–942, 2009.

[25] R. Tron and K. Daniilidis, "An optimization approach to bearing-only visual homing with applications to a 2-D unicycle model," in *2014 IEEE International Conference on Robotics and Automation (ICRA)*, pp. 4235–4242, IEEE, 2014.

[26] H. Sert, A. Kökösy, and W. Perruquetti, "A single landmark based localization algorithm for non-holonomic mobile robots," in *Robotics and Automation (ICRA), 2011 IEEE International Conference on*, pp. 293–298, IEEE, 2011.

[27] "Image database using multiple cameras." `http://www.sc.iitb.ac.in/~leena/vh/Image_database/`, 2015.

[28] A. Vardy and R. Moller, "Biologically Plausible Visual Homing Methods based on Optical Flow Techniques," *Connection Science, Special issue:Navigation*, vol. 17, no. 1-2, pp. 47–89, 2005.